JB
Journals.ASM.org

Activation of CpxRA in *Haemophilus ducreyi* Primarily Inhibits the Expression of Its Targets, Including Major Virulence Determinants

Dharanesh Gangaiah,[a] Xinjun Zhang,[d] Kate R. Fortney,[a] Beth Baker,[f] Yunlong Liu,[d] Robert S. Munson, Jr.,[f,g] Stanley M. Spinola[a,b,c,e]

Departments of Microbiology and Immunology,[a] Medicine,[b] Pathology and Laboratory Medicine,[c] and Medical and Molecular Genetics[d] and Center for Immunobiology,[e] Indiana University School of Medicine, Indianapolis, Indiana, USA; Center for Microbial Pathogenesis, Nationwide Children's Hospital,[f] and Department of Pediatrics, The Ohio State University College of Medicine,[g] Columbus, Ohio, USA

***Haemophilus ducreyi* causes chancroid, a genital ulcer disease that facilitates the transmission of human immunodeficiency virus type 1. In humans, *H. ducreyi* is surrounded by phagocytes and must adapt to a hostile environment to survive. To sense and respond to environmental cues, bacteria frequently use two-component signal transduction (2CST) systems. The only obvious 2CST system in *H. ducreyi* is CpxRA; CpxR is a response regulator, and CpxA is a sensor kinase. Previous studies by Hansen and coworkers showed that CpxR directly represses the expression of *dsrA*, the *lspB-lspA2* operon, and the *flp* operon, which are required for virulence in humans. They further showed that CpxA functions predominantly as a phosphatase *in vitro* to maintain the expression of virulence determinants. Since a *cpxA* mutant is avirulent while a *cpxR* mutant is fully virulent in humans, CpxA also likely functions predominantly as a phosphatase *in vivo*. To better understand the role of *H. ducreyi* CpxRA in controlling virulence determinants, here we defined genes potentially regulated by CpxRA by using RNA-Seq. Activation of CpxR by deletion of *cpxA* repressed nearly 70% of its targets, including seven established virulence determinants. Inactivation of CpxR by deletion of *cpxR* differentially regulated few genes and increased the expression of one virulence determinant. We identified a CpxR binding motif that was enriched in downregulated but not upregulated targets. These data reinforce the hypothesis that CpxA phosphatase activity plays a critical role in controlling *H. ducreyi* virulence *in vivo*. Characterization of the downregulated genes may offer new insights into pathogenesis.**

Haemophilus ducreyi is a Gram-negative facultative anaerobe that causes chancroid, a genital ulcer disease characterized by painful genital ulcers and regional lymphadenopathy. While uncommon in the United States, chancroid is endemic in the developing countries of Africa, Asia, and Latin America and is a risk factor for the acquisition and transmission of human immunodeficiency virus type 1 (HIV-1) (1). Because of syndromic management of genital ulcer disease, the global prevalence of chancroid is currently undefined (2). In the South Pacific, *H. ducreyi* is also reported to cause a chronic lower limb ulceration syndrome that is not sexually transmitted (3–5).

H. ducreyi is an obligate human pathogen with no known environmental reservoirs. The development of a human infection model has significantly contributed to our understanding of *H. ducreyi* pathogenesis (6). During experimental and natural infections, *H. ducreyi* resides in an abscess composed of neutrophils and macrophages (7, 8). Thus, *H. ducreyi* is likely exposed to multiple stresses in the human host, including antimicrobial peptides, the hypoxic environment of an abscess, and nutrient limitation. The fact that *H. ducreyi* is a successful pathogen suggests that this organism harbors mechanisms to sense and respond to stresses imposed by the host.

Gram-negative bacteria often use two-component signal transduction (2CST) systems to sense, respond to, and adapt to extracellular stresses. The *Escherichia coli* Cpx 2CST system allows bacteria to sense and respond to stresses affecting the cell envelope (9–12). The Cpx 2CST system consists of the histidine kinase CpxA and the response regulator CpxR. In response to envelope stress, CpxA autophosphorylates on a conserved histidine residue; phosphorylated CpxA donates its phosphoryl group to CpxR at a conserved aspartic acid residue (9). By binding to conserved recognition sequences, phosphorylated CpxR regulates the transcription of many genes involved in alleviating envelope stress in *E. coli* (13–15). In addition to kinase activity, CpxA also possesses CpxR-specific phosphatase activity (9). When grown in media containing glucose, CpxR accepts phosphoryl groups from acetyl phosphate (AcP) (16). When a *cpxA* deletion mutant is grown in the presence of glucose, CpxR is not readily dephosphorylated and the system is constitutively activated (16, 17).

The *H. ducreyi* genome (GenBank accession no. AE017143) contains homologues of CpxRA, which is the only obvious intact 2CST system in the genome. *H. ducreyi* is a fastidious organism and can only be grown in media containing glucose. Compared to its parent, a *cpxR* deletion mutant increases the transcription and expression of the *lspB-lspA2* operon, which encodes proteins involved in the resistance of *H. ducreyi* to phagocytosis (18). The *lspB-lspA2* promoter region contains putative CpxR recognition sequences, and recombinant CpxR binds to the promoter region of *lspB-lspA2* in electrophoretic mobility shift assays. Taken together, these observations support the hypothesis that CpxR directly represses the expression of this operon (19). In contrast, a *cpxA* deletion mutant, which expresses the same level of CpxR as its parent, downregulates transcription from the *lspB-lspA2* promoter (20, 21). Thus, CpxA regulates CpxR. If binding to the

Received 3 May 2013 Accepted 29 May 2013
Published ahead of print 31 May 2013
Address correspondence to Dharanesh Gangaiah, dgangaia@iupui.edu.
Supplemental material for this article may be found at http://dx.doi.org/10.1128/JB.00372-13.

doi:10.1128/JB.00372-13

TABLE 1 Bacterial strains and plasmids used in this study

Strain or plasmid	Description	Source or reference
E. coli DH5α	Strain used for general cloning procedures	Invitrogen
H. ducreyi strains		
35000HP	Human-passaged variant of strain 35000; parental strain	56
35000HPΔ*cpxR*	35000HP*cpxR* in-frame deletion mutant containing a chloramphenicol resistance cartridge	19
35000HPΔ*cpxA*	35000HP*cpxA* unmarked, in-frame deletion mutant	20
Plasmids		
pRB157	pLS88 derivative containing an ΩAmp cartridge, followed by a BglII site for insertion of promoter sequences and a promoterless GFP cassette derived from pGreenTIR	20
pKF1	pRB157 derivative containing the *lspB* promoter region	20
pKF2	pRB157 derivative containing the *dsrA* promoter region	20
pDG2	pRB157 derivative containing the *HD0182* promoter region	This study
pDG3	pRB157 derivative containing the *fimA* promoter region	This study
pDG4	pRB157 derivative containing the *HD0427* promoter region	This study
pDG5	pRB157 derivative containing the *HD1123* promoter region	This study
pDG6	pRB157 derivative containing the *HD1278* promoter region	This study
pDG7	pRB157 derivative containing the *fis* promoter region	This study

lspB-lspA2 promoter requires phospho-CpxR, then CpxA functions in *H. ducreyi* as if it were a net phosphatase (21), similar to what occurs when an *E. coli cpxA* deletion mutant is grown in media containing glucose (16, 17).

A previous microarray analysis showed that activation of the Cpx 2CST system by deletion of *cpxA* also downregulates the transcription of *dsrA* and the *flp* operon, which are both required for the virulence of *H. ducreyi* in humans (18); recombinant CpxR also binds to the *dsrA* and *flp* promoter regions in electrophoretic mobility shift assays, suggesting that phospho-CpxR also directly represses transcription from these promoters (18). Compared to its parent strain, a *cpxA* deletion mutant is avirulent (20), while a *cpxR* deletion mutant is fully virulent in human inoculation experiments (21). Taken together, these finding imply that CpxA likely functions primarily as a net phosphatase during infection in humans.

To better understand the role of the Cpx 2CST system in *H. ducreyi* pathogenesis, here we defined genes potentially regulated by CpxR in *H. ducreyi* by using RNA-Seq. To this end, we compared the RNA-Seq-defined transcriptomes of the parent, a *cpxA* mutant, and a *cpxR* mutant at different growth phases. We show that activation of the Cpx 2CST system by deletion of *cpxA* repressed the transcription of the majority of its targets, including seven known virulence determinants, and identified a CpxR binding motif that was enriched in the downregulated targets. In contrast, inactivation of the Cpx 2CST system by deletion of *cpxR* differentially regulated only a small number of genes and upregulated one gene encoding a known virulence determinant. These results are consistent with our previous observations that the *cpxA* mutant is fully attenuated while the *cpxR* mutant is fully virulent in humans and support the model in which CpxA acts primarily as a net phosphatase during *H. ducreyi* infection. Characterization of the downregulated genes may offer new insights into *H. ducreyi* pathogenesis.

MATERIALS AND METHODS

Bacterial strains, plasmids, and culture conditions. The bacterial strains and plasmids used in this study are listed in Table 1. The *H. ducreyi* strains were grown on chocolate agar plates supplemented with 1% IsoVitaleX at 33°C with 5% CO_2 or in gonococcal (GC) broth supplemented with 5% fetal bovine serum (HyClone), 1% IsoVitaleX, and 50 μg/ml of hemin (Aldrich Chemical Co.) at 33°C. For RNA isolation, *H. ducreyi* strains were grown to the mid-log (optical density at 600 nm [OD_{660}] of 0.2), transition (OD_{660} of 0.31), or early stationary phase (referred to here as stationary phase; OD_{660} of 0.35) in GC broth (see Fig. S1 in the supplemental material). *E. coli* strains were grown in Luria-Bertani medium at 37°C. When necessary, media were supplemented with streptomycin (50 μg/ml for *H. ducreyi*, 100 μg/ml for *E. coli*).

RNA isolation and quality assessment. Total RNA was extracted from 35000HP, 35000HPΔ*cpxA* (20), and 35000HPΔ*cpxR* (19) in the mid-log, transition, and stationary growth phases using TRIzol reagent (Invitrogen) according to the manufacturer's protocol. RNA isolation was performed on four independent bacterial cultures for each strain in each growth phase. RNA was treated twice with the TURBO DNA-free DNase (Ambion). The integrity and the concentration of RNA were determined using the Agilent 2100 Bioanalyzer (Agilent Technologies) and the NanoDrop ND-1000 spectrophotometer (Thermo Scientific), respectively. The efficacy of DNase treatment was confirmed by reverse transcriptase PCR (RT-PCR) analysis of *dnaE* with the primer pair P1/P2 (see Table S1 in the supplemental material) and the QuantiTect SYBR green RT-PCR kit (Qiagen).

mRNA enrichment. The removal of 23S, 16S, and 5S rRNA from total RNA was performed with the Ribo-Zero Magnetic kit (Gram-negative bacteria) (Epicenter Biotechnologies) by following the manufacturer's instructions. The removal of rRNA from total RNA was confirmed by the Agilent 2100 Bioanalyzer.

Preparation of RNA-Seq libraries and sequencing. The TruSeq RNA sample preparation kit (Illumina, Inc.) was used to prepare RNA-Seq libraries by following the manufacturer's instructions. Briefly, approximately 10 to 100 ng of the enriched mRNA was fragmented and randomly primed for first-strand cDNA synthesis, followed by second-strand cDNA synthesis. The double-stranded cDNA was end repaired, adenylated, and ligated to adapters. The adapter-ligated cDNA library was then PCR enriched. Finally, the enriched RNA-Seq library was validated with the Agilent 2100 Bioanalyzer and quantitative RT-PCR (qRT-PCR). Clusters were generated on the cBOT automated cluster-generating system with the TruSeq PE Cluster kit (Illumina). Libraries were sequenced with the Illumina HiSeq 2500 sequencer with the TruSeq SBS kit (Illumina) for paired-end sequencing with read lengths of 100 bp in the Biomedical

Genomics Core facility at Nationwide Children's Hospital (Columbus, OH). Image analysis and base calling were performed with the HiSeq Control software and the Real Time Analysis software. Demultiplexing was performed with the Illumina CASAVA software.

Sequence mapping and quantification of transcript levels. The sequenced reads were mapped to the *H. ducreyi* 35000HP genome (GenBank accession no. AE017143) with the Burrows-Wheeler Alignment tool BWA (22), allowing up to two base mismatches. Reads that failed to map to any gene in the chromosome and reads that mapped to multiple locations in the genome were removed before quantifying the transcript levels. The total number of reads corresponding to the coding region of each gene was determined with the NGSUtils suite (23).

Identification of differentially expressed genes. Differential expression of genes across different strains and growth phases was determined with edgeR software, a Bioconductor package for the differential expression analysis of digital gene expression data based on a negative binomial distribution (24). Because many genes were tested, we used a prespecified false-discovery rate (FDR) of ≤0.1 as the criterion for differential transcript expression; the FDR is less stringent than determining a familywise type 1 error with adjustment for multiple comparisons (25). We also chose a 2-fold change as a threshold for differential transcript expression, reasoning that this may favor the identification of genes that are biologically more significant than those with smaller changes. The differentially expressed genes were organized into known or putative operons with the computationally predicted operon structures from DOOR (Database for prOkaryotic OpeRons) (26). The differentially expressed genes or operons were functionally classified by using the annotations and pathway information from the sequenced *H. ducreyi* genome (R. S. Munson, Jr., et al., 2004, unpublished data), EcoCyc (27), and KEGG (28). We also determined if any biological pathways were enriched among the genes or operons differentially expressed in the *cpxA* and *cpxR* mutants compared to 35000HP by using the pathway annotations from BioCyc (29). A pathway was defined as enriched if the percentage of its differentially expressed genes was higher than that of all of the other pathways and if the *P* value for the pathway was <0.05 by Fisher's exact test. We also used the functional annotation-clustering algorithm of the DAVID (Database for Annotation, Visualization, and Integrated Discovery) bioinformatics resources (http://david.abcc.ncifcrf.gov/) to identify the biological pathways enriched in the *cpxA* and *cpxR* mutants relative to 35000HP (30). A pathway was considered enriched if the Fisher's exact *P* value for the cluster was < 0.05, the enrichment score for the cluster was greater than two, and the cluster involved greater than 5% of the genes on the submitted list (12).

qRT-PCR. qRT-PCR was performed with the QuantiTect SYBR green RT-PCR kit (Qiagen) in an ABI Prism 7000 sequence detection system (Applied Biosystems). The primer pairs P1/P2 to P35/P36 were used to amplify internal gene-specific fragments ranging from 70 to 200 bp (see Table S1 in the supplemental material). For all qRT-PCR experiments, the amplification efficiency was determined for each primer pair; all primer pairs had greater than 95% efficiency. The expression levels of target genes were normalized to that of *dnaE* with the primer pair P1/P2. The fold change in expression was calculated as follows: $[\text{ratio} = (E_{\text{target}})^{\Delta CT\text{target (35000HP}\Delta cpxA\text{-35000HP}\Delta cpxR)} / (E_{\text{reference}})^{\Delta CT\text{reference (35000HP}\Delta cpxA\text{-35000HP}\Delta cpxR)}]$, where E is the amplification efficiency (equal to $10^{-1/\text{slope}}$) and ΔC_T is the change in cycle threshold (20).

Reporter assays. Reporter assays were performed as previously described (20). Approximately 200 bp of the *HD0182*, *fimA*, *HD0427*, *HD1123*, *HD1278*, and *fis* promoter regions were amplified by PCR with primer pairs P37/P38, P39/P40, P41/P42, P43/P44, P45/P46, and P47/P48, respectively (see Table S1 in the supplemental material). The amplified PCR products were ligated to pRB157 by using the BglII restriction site preceding a promoterless green fluorescent protein (GFP) cassette. The orientation of the insert with respect to the *gfp* cassette was confirmed by PCR with a promoter specific forward primer and the reverse primer P49 that hybridized to a region of the *gfp* cassette downstream of the BglII site. The final construct containing the promoter region preceding the *gfp* cassette was confirmed by sequencing. The reporter constructs were then electroporated into 35000HP, 35000HPΔ*cpxA*, and 35000HPΔ*cpxR*. Reporter strains generated previously were used for the analysis of the *lspB* and *dsrA* promoter activity (20). Whole-cell lysates were prepared from each transformant harvested at the stationary growth phase and analyzed by Western blot assays with monoclonal antibodies specific to GFP (Clontech) and the peptidoglycan-associated protein (PAL) (20). For each strain, the level of expression of GFP normalized to PAL was determined by densitometry with ImageJ software (31). Densitometry data were analyzed by two-tailed Student *t* test; a *P* value of <0.05 was considered statistically significant.

Identification of a putative CpxR binding motif. The Multiple EM for Motif Elicitation (MEME) algorithm was used for *de novo* identification of the CpxR binding consensus sequence in *H. ducreyi* (32). Because of the lack of experimentally validated CpxR-dependent promoter motifs for *H. ducreyi*, the 450-bp upstream promoter regions of the 66 downregulated genes or operons were used for *de novo* motif identification by the MEME algorithm restricting the motif length to 15 to 50 bp. A similar analysis was also performed on the upregulated genes or operons. The identified motif was then encoded as a position-specific scoring matrix (PSSM). To test the significance of the discovered motif, matching scores were calculated on the basis of the promoter sequence and the motif feature characterized by the PSSM by using a previously published strategy (33). The score cutoff was determined by maximizing the enrichment of identified motif in the promoter regions of downregulated genes/operons compared to the promoter regions of unaffected genes.

Site-directed mutagenesis of the *lspB* promoter. Mutations were introduced into the *lspB* promoter region in pKF1 with the QuikChange II XL (Agilent Technologies) site-directed mutagenesis kit by following the manufacturer's instructions. The *lspB* promoter in pKF1 contains four putative CpxR binding sites. The first two nucleotides in the first conserved region of each motif were mutated from G to T and from T to G. Mutagenic primers were designed with the QuikChange Primer Design Program (Agilent Technologies). The primer pairs P50/P51, P52/P53, P54/P55, and P56/P57 were used to mutagenize binding motifs 1 to 4, respectively (see Table S1 in the supplemental material). All of the mutations were confirmed by sequencing. The plasmids containing the mutated *lspB* promoter sequences were electroporated into 35000HPΔ*cpxA* and 35000HPΔ*cpxR*; the transformants were grown to mid-log phase, and the GFP/PAL expression ratio was measured as described above. Densitometry data were analyzed by two-tailed Student *t* test. Following Bonferroni adjustment, a *P* value of <0.0125 was considered statistically significant.

RESULTS

Transcriptome analysis. In *H. ducreyi*, activation of the CpxRA system represses the transcription of several virulence determinants and cripples the ability of the organism to infect humans (18, 20). To more precisely define the role of the Cpx-regulated genes in virulence, we compared the transcriptomes of 35000HP, which has physiological levels of Cpx activation, 35000HPΔ*cpxA*, which has a constitutively activated Cpx system due to loss of CpxA phosphatase activity, and 35000HPΔ*cpxR*, which has no Cpx activity (18). We grew the strains to the mid-log, transition, and stationary growth phases (see Fig. S1 in the supplemental material), isolated RNA, and determined their transcriptomes with RNA-Seq.

Four biological replicates were included for each strain in each growth phase, summing to a total of 36 samples. The percentage of total reads aligned with the reference genome from all strains, growth phases, and replicates ranged from 98.5 to 99.3% (see Table S2 in the supplemental material). The percentage of reads aligned with the coding regions ranged from 63.9 to 83.6% (see

Table S2). The average coverage per nucleotide ranged from 1.5 to 22.9 (see Table S2). As expected, approximately equal percentages of reads were found in the sense and antisense strands (see Table S2). The coefficients of determination (R^2) between the samples from all strains, growth phases, and replicates ranged from 0.98 to 0.99, showing that there was high reproducibility of the RNA-Seq data.

Identification of genes regulated by CpxRA. To identify genes potentially regulated by CpxRA in *H. ducreyi*, we calculated the fold change in the expression of genes in the *cpxA* mutant relative to the *cpxR* mutant and the fold change in the expression of genes in the *cpxA* and *cpxR* mutants relative to the parent. As discussed in Materials and Methods, we used an FDR of ≤0.1 and a 2-fold change as criteria for differential transcript expression. All genes considered differentially regulated by these criteria had *P* values of <0.01. Where appropriate, we grouped the differentially regulated genes into operons so that individual genes within a transcriptional unit were reported as one target.

As expected, comparison of 35000HPΔ*cpxA* to 35000HP Δ*cpxR* identified the most differences, with 86, 68, and 94 targets differentially regulated by the Cpx 2CST system in the mid-log, transition, and stationary growth phases, respectively; 63, 59, and 70% of these targets were downregulated (see Fig. S2 and Table S3 in the supplemental material). Comparison of 35000HPΔ*cpxA* to 35000HP identified 52, 43, and 78 targets differentially regulated in the mid-log, transition, and stationary growth phases, respectively; 76, 82, and 69% of these targets were downregulated (see Fig. S2 and Table S4 in the supplemental material). Comparison of 35000HP to 35000HPΔ*cpxR* identified only 12, 7, and 23 targets differentially regulated by the Cpx 2CST system in the mid-log, transition, and stationary growth phases, respectively; 33, 29, and 61% of these targets were downregulated (see Fig. S2 and Table S5 in the supplemental material). For the majority of the differentially regulated targets in all comparisons, the fold change was maximal in the stationary phase, intermediate in the mid-log phase, and lowest in the transition phase (see Tables S3, S4, and S5 in the supplemental material). These results suggest that the Cpx 2CST system is activated in a growth phase-dependent manner; most of the differential regulation occurs in the stationary phase.

To identify the overlap between the genes or operons that were differentially regulated by activation and inactivation of the Cpx 2CST system, we calculated the fold changes in the expression of genes in 35000HPΔ*cpxA* and 35000HPΔ*cpxR* relative to 35000HP and plotted the $\log_{10}$-transformed fold changes in 35000HP Δ*cpxA*/35000HP against 35000HPΔ*cpxR*/35000HP. This analysis clearly shows that activation of the system by deletion of *cpxA* serves to repress many targets, while repression of the system by deletion of *cpxR* increases the expression of a much smaller number of targets (Fig. 1). Few genes or operons were differentially regulated in both the *cpxA* and *cpxR* mutants relative to parent, suggesting that activation and inactivation of the system control unique sets of genes (Fig. 1).

qRT-PCR confirms the fold changes estimated by RNA-Seq. Since the most profound differential regulation was noted in the 35000HPΔ*cpxA*-versus-35000HPΔ*cpxR* comparison in the stationary phase, we concentrated on this data set for the remainder of this study. We validated the differentially regulated targets by qRT-PCR. The targets were divided into three groups on the basis of their expression levels (high, medium, and low); the expression levels were determined by the read abundance,

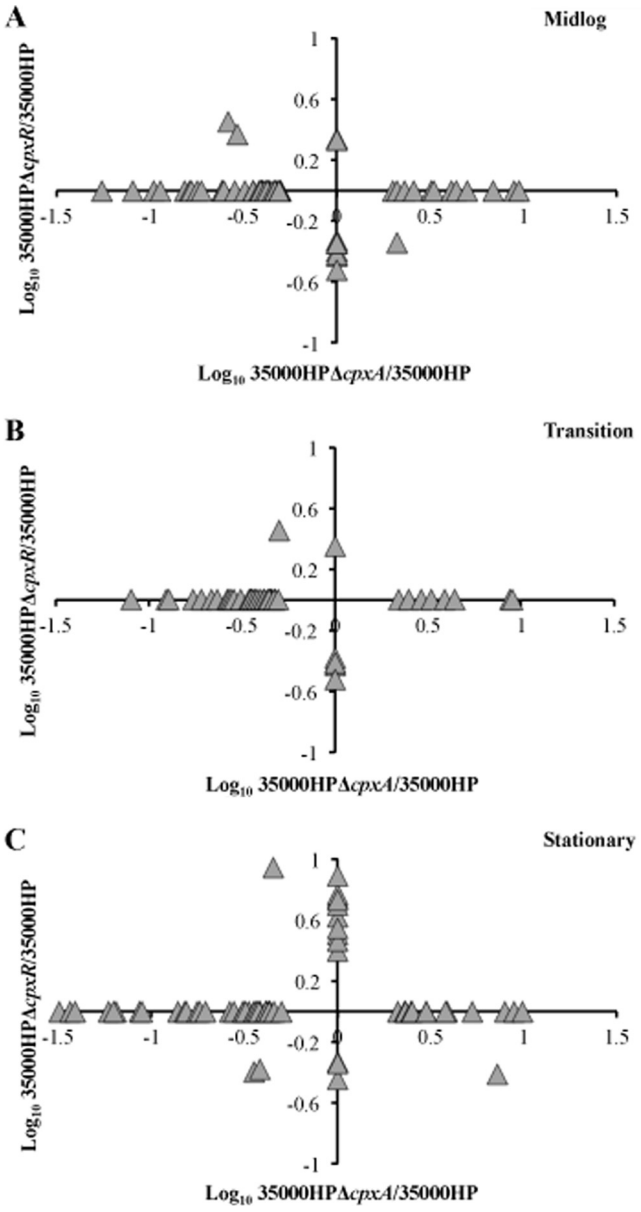

FIG 1 Scatter plots showing fold changes in the expression of genes or operons differentially expressed in 35000HPΔ*cpxA* and 35000HPΔ*cpxR* compared to 35000HP. The scatter plots were generated by plotting the $\log_{10}$-transformed fold changes in 35000HPΔ*cpxA* versus 35000HP against 35000HPΔ*cpxR* versus 35000HP at different growth phases. Each triangle in the graph indicates a single gene or operon.

which is the average log-transformed concentration for a gene across 35000HPΔ*cpxA* and 35000HPΔ*cpxR* (Fig. 2A). Genes from each expression level were then subgrouped into up- and downregulated genes (Fig. 2A). The up- and downregulated genes were stratified on the basis of their fold changes (2 to 4.9, 5 to 14.9, 15 to 29.9, and 30 to 60) (Fig. 2A). Representative genes were selected arbitrarily from each category; a total of 16 genes were evaluated by qRT-PCR. Our findings showed that the qRT-PCR analysis confirmed the expression of 15/16 targets identified by RNA-Seq (Fig. 2A). In general, the fold changes derived from RNA-Seq were in good agreement with the fold changes derived from qRT-PCR,

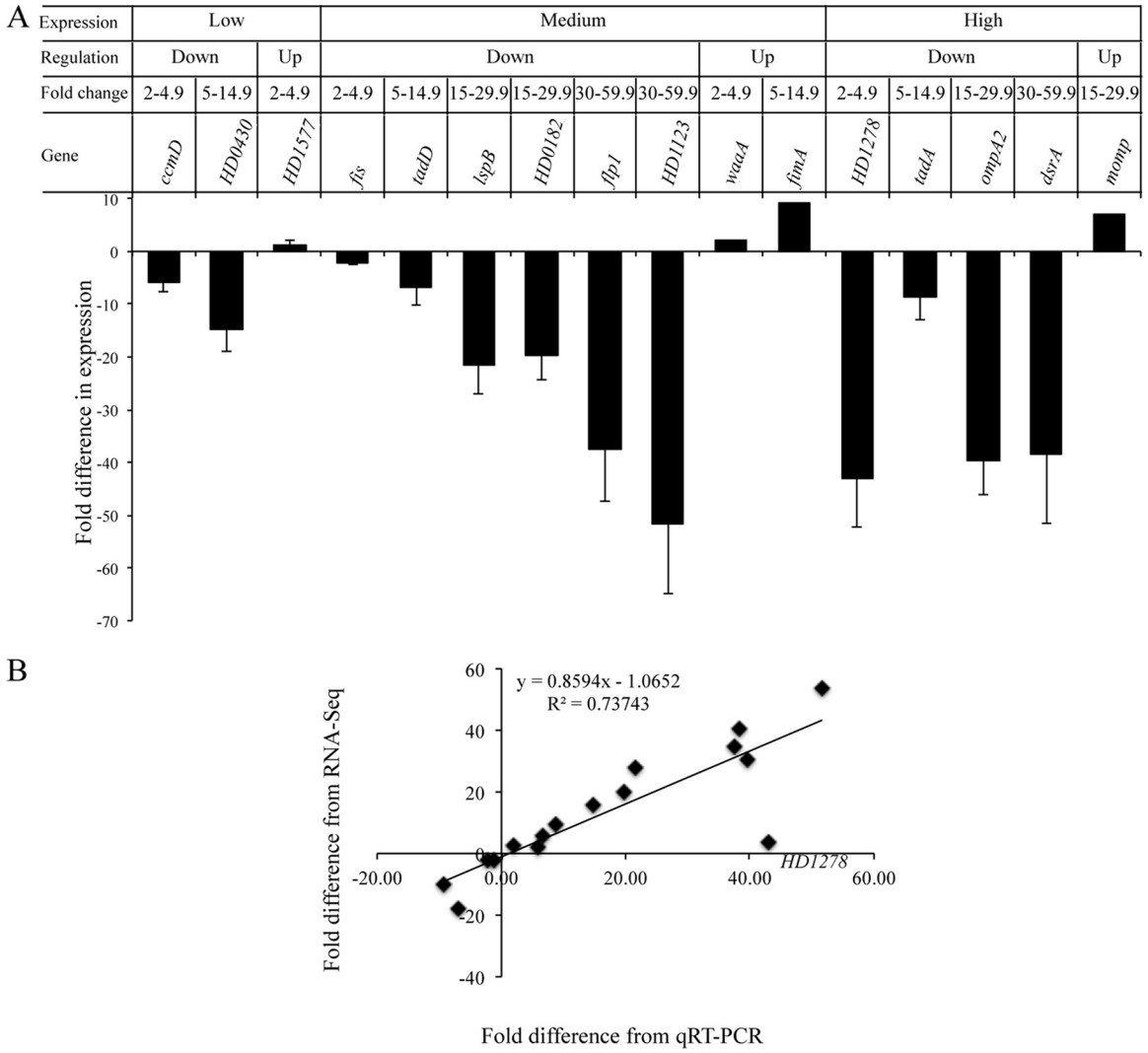

FIG 2 qRT-PCR validation of the RNA-Seq data. (A) Fold changes in the expression of target genes in 35000HPΔ*cpxA* relative to 35000HPΔ*cpxR* in the stationary phase. The criteria used for selecting the targets for qRT-PCR validation are outlined at the top. The expression levels of target genes were normalized to that of *dnaE*. The data represent the mean ± SD from four independent experiments. (B) Correlation between the fold changes derived from qRT-PCR and RNA-Seq. The gene *HD1278*, for which the fold changes derived from the qRT-PCR data were not in agreement with the fold changes derived from the RNA-Seq data, is labeled on the graph.

except for *HD1278*, which was 3.7-fold downregulated by RNA-Seq and 43-fold downregulated by qRT-PCR (Fig. 2B); the reason for this discrepancy is unclear.

Reporter assays confirm the CpxR regulation of *HD0182*, *HD0427*, *HD1123*, *lspB*, and *dsrA*. We determined the Cpx dependence of selected target gene promoters in 35000HP, 35000HPΔ*cpxA*, and 35000HPΔ*cpxR* grown to the mid-log, transition, and stationary phases. As the most profound differences were found in the stationary phase, these data are presented in Fig. 3. The expression levels of *HD0182*, *HD0427*, *HD1123*, *lspB*, and *dsrA* were downregulated in the *cpxA* mutant compared to its parent and the *cpxR* mutant, suggesting CpxR regulation of these targets (Fig. 3A and B). However, the expression of *fimA*, *fis*, and *HD1278* was unaltered in 35000HP, 35000HPΔ*cpxA*, and 35000HPΔ*cpxR* (Fig. 3A and B). A previous study showed that recombinant CpxR does not bind to the *fimA* promoter region (18); thus, the regulation of *fimA* is likely indirect. RNA-Seq and qRT-PCR showed only 2.0- and 2.4-fold upregulation, respectively, of *fis* transcripts in the *cpxA* mutant compared to the *cpxR* mutant; the GFP reporter assay may not be sensitive enough to detect this level of upregulation. Alternatively, the Cpx 2CST system may regulate the expression of *fimA*, *fis*, and *HD1278* at the posttranscriptional level. Overall, the results of the reporter assays correlated well with the RNA-Seq and qRT-PCR data.

Activation of the Cpx 2CST system downregulates several *H. ducreyi* virulence determinants required for infection of humans. We assessed if activation of the Cpx 2CST system affects the expression of genes tested for virulence in humans (Table 2). Activation of the Cpx 2CST system by deletion of *cpxA* downregulated the expression of genes in the *flp-tad* and *lspB-lspA2* operons, *dsrA*, *ncaA*, and *hgbA*, which are all absolutely required for abscess formation in human volunteers (Table 2) (6, 34). Activation of the Cpx 2CST system downregulated *dltA*, which is partially required for abscess formation (Table 2) (6). These genes all encode se-

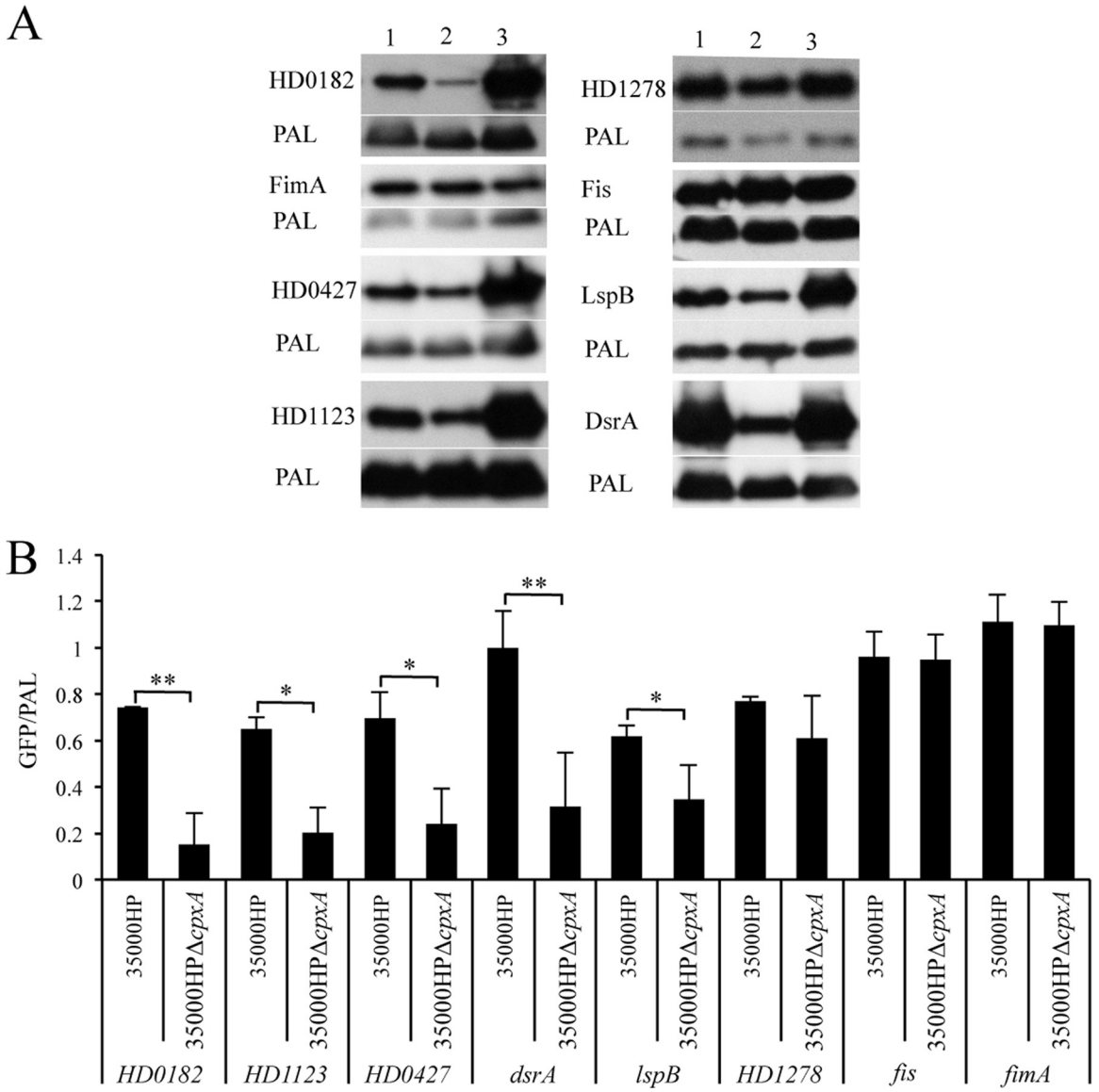

FIG 3 Promoter-reporter analysis of the Cpx targets identified by RNA-Seq. (A) The *in vivo* transcriptional activity of the Cpx-regulated promoters in 35000HP (lane 1), 35000HPΔ*cpxA* (lane 2), and 35000HPΔ*cpxR* (lane 3) grown to the stationary phase. For assessment of promoter activity, whole-cell lysates of *H. ducreyi* strains containing the reporter constructs were probed with an anti-GFP monoclonal antibody and anti-PAL monoclonal antibody 3B9, which served as a loading control. (B) Densitometry analysis of the Western blot assays in panel A. The Cpx dependence of target promoters was assessed by normalizing the GFP/PAL ratio in 35000HP and 35000HPΔ*cpxA* to that in 35000HPΔ*cpxR*, which was set to a value of 1. The data are means ± standard deviations from three independent experiments. *, $P < 0.05$; **, $P < 0.01$.

creted or outer membrane proteins (OMPs) that play direct roles in virulence such as nutrient acquisition, adherence, and resistance to phagocytic and serum killing. In contrast, deletion of *cpxR* had no effect on the transcription of virulence determinants, except for upregulation of *lspB-lspA2*. Surprisingly, deletion of *cpxR* downregulated *dltA* in all phases of growth (Table 2; see Table S5 in the supplemental material). These data are consistent with the attenuation of the *cpxA* mutant and the virulence of the *cpxR* mutant in humans and support the hypothesis that *cpxA* acts as a net phosphatase *in vivo* (18, 20).

The transcription of *pal*, *sapBC*, and *hfq*, which are also absolutely required for virulence, and *fgbA*, *wecA*, *sapA*, *luxS*, and *csrA*, which are partially required for virulence, was not affected by activation of the Cpx 2CST system (6, 35–37) (unpublished data; Table 2). *pal* encodes a structural component of the cell envelope and may have an indirect role in virulence (36, 38). *sapA* and *sapBC* encode periplasmic and inner membrane proteins that facilitate the uptake and degradation of antimicrobial peptides (36, 39). *hfq* and *csrA* encode cytoplasmic proteins that are involved primarily in posttranscriptional regulation. *fgbA* encodes an OMP that binds fibrinogen in ligand blot assays (40). *wecA* encodes the first enzyme involved in the synthesis of the enterobacterial common antigen; however, the glycoconjugate synthesized by this pathway in *H. ducreyi* has not been identified (41). *luxS* encodes an enzyme that produces an autoinducer-2-like molecule (35) Thus, virulence determinants not regulated by the Cpx 2CST sys-

TABLE 2 Regulation of genes tested for virulence in humans by the Cpx 2CST system

Human challenge model[a]	Function	35000HPΔ*cpxA*/ 35000HP[b]	35000HPΔ*cpxR*/ 35000HP[c]
Attenuated			
flp1-flp2-flp3	Adherence and microcolony formation	−31.3	—[d]
dsrA	Major role in serum resistance	−27.4	—
lspA1, *lspA2*	Escape from phagocytosis	−15.4	2.8
ncaA	Collagen binding	−7.2	—
tadA	Adherence and microcolony formation	−6.9	—
hgbA	Heme and/or iron uptake	−2.6	—
pal	Outer membrane stability	—	—
sapBC	Resistance to antimicrobial peptides	—	—
hfq	RNA-binding chaperone	—	—
Partially attenuated			
dltA	Partial role in serum resistance	−2.8	−2.7
wecA	Initiates synthesis of putative glycoconjugate	—	—
luxS	Quorum sensing	—	—
fgbA	Fibrinogen binding	—	—
sapA	Resistance to antimicrobial peptides	—	—
csrA	Posttranscriptional regulation	—	—
Virulent			
hhdB[e]	Lysis of fibroblasts	−16.9	—
ompP2A, *ompP2B*	Encode classical trimeric porins	−11.2 (*ompP2A*), 15.9 (*ompP2B*)	—
sodC	Detoxifies ROS[f]	−2.4	—
momp	OmpA homolog; minor role in fibronectin binding	7.2	—
losB	Extends LOS[g] beyond KDO[h]-triheptose-glucose	—	—
lst	Adds sialic acid to LOS	—	—
cdtC[e]	Toxic for T cells, epithelial cells, and fibroblasts	—	—
ftpA	Pilus	—	—
tdX/*tdhA*	Heme uptake	—	—
glu	Adds glucose to KDO-triheptose LOS core	—	—
ompP4	Outer membrane lipoprotein	—	—
neuA	Enables sialic acid addition to LOS	—	—

[a] Mutants of genes that have been tested in human volunteers and classified as attenuated, partially attenuated, or virulent.
[b] Fold change in 35000HPΔ*cpxA* relative to 35000HP in stationary phase.
[c] Fold change in 35000HPΔ*cpxR* relative to 35000HP in stationary phase.
[d] —, no change in expression.
[e] *hhdB cdtC* double mutant is also virulent in humans.
[f] ROS, reactive oxygen species.
[g] LOS, lipooligosaccharide.
[h] KDO, 2-keto-3-deoxyoctulosonic acid.

tem were generally those that were not secreted extracellularly or incorporated into the outer envelope.

Activation of the Cpx 2CST system downregulated the expression of *hhdB*, *ompP2A*, and *sodC*, which are not required for virulence in humans (Table 2) (6). *sodC* encodes a periplasmic copper-zinc superoxide dismutase, *hhdB* is involved in the secretion of hemolysin, and *ompP2A* encodes a porin (42–44). Thus, downregulation of the expression of OMPs or secreted proteins by CpxRA does not necessarily imply a role in virulence. Activation of the Cpx 2CST system upregulated the expression of *ompP2B*, *momp*, *neuA*, and *lst*, which are also not required for virulence (Table 2) (6, 45). *neuA* and *lst* encode enzymes involved with sialylation of lipooligosaccharide (45), while the remaining genes encode structural OMPs.

Functional classification of genes or operons differentially expressed in the *cpxA* mutant compared to the *cpxR* mutant. With the annotations and pathway information from the sequenced *H. ducreyi* genome (Munson et al., 2004, unpublished), EcoCyc (27), and KEGG (28), the identified Cpx targets were classified into several functional categories, including amino acid biosynthesis, cell surface structures and associated proteins, cofactor biosynthesis, generation of precursor metabolites and energy, membrane transport and uptake, regulation and cell signaling, stress survival, translation, and hypothetical proteins (Table 3). The most notable biologically significant transcriptome changes in the *cpxA* mutant compared to *cpxR* mutant in the stationary phase are described below.

Amino acid biosynthesis. Activation of the Cpx 2CST system downregulated the expression of homologues of genes involved in the biosynthesis of cysteine (*cysK*) and selenocysteine (*selD*) and upregulated the expression of homologues of genes involved in arginine biosynthesis (*argC-argB*) and regulation (*argR*) (Table 4; see Table S3 in the supplemental material).

Cell surface structures and associated proteins. The Cpx 2CST system downregulated the expression of 14 genes or operons encoding or predicted to encode OMPs, secreted proteins, or

TABLE 3 Functional classification of genes or operons differentially regulated by activation or inactivation of the Cpx 2CST system in *H. ducreyi*

Parameter	Mid-log			Transition			Stationary		
	35000HP-Δ*cpxA*/ 35000HP-Δ*cpxR*[a]	35000HP-Δ*cpxA*/ 35000HP[b]	35000HP-Δ*cpxR*/ 35000HP[c]	35000HP-Δ*cpxA*/ 35000HP-Δ*cpxR*[a]	35000HP-Δ*cpxA*/ 35000HP[b]	35000HP-Δ*cpxR*/ 35000HP[c]	35000HP-Δ*cpxA*/ 35000HP-Δ*cpxR*[a]	35000HP-Δ*cpxA*/ 35000HP[b]	35000HP-Δ*cpxR*/ 35000HP[c]
% Downregulated targets	63	76	67	59	82	71	70	69	39
% Upregulated targets	37	24	33	41	18	29	30	31	61
Functional categories:									
Amino acid biosynthesis	2	1	—[d]	3	1	—	3	2	—
Cell surface structures and associated proteins	21	18	5	19	13	2	30	23	11
Cell wall biosynthesis and remodeling	2	—	—	3	—	—	1	—	—
Cofactor biosynthesis	2	2	—	1	1	—	4	2	1
Degradation/assimilation/utilization	1	1	0	1	1	0	1	1	0
DNA replication, recombination, and repair	1	1	—	1	—	—	—	—	—
Fatty acid biosynthesis	—	—	—	—	—	—	1	1	—
Generation of precursor metabolites and energy	10	7	1	8	6	1	7	7	—
Hypothetical proteins	22	9	3	16	11	3	16	20	5
Lipid biosynthesis	1	1	—	—	—	—	—	1	—
Membrane transport/uptake	11	8	3	9	3	1	10	7	2
Nucleoside and nucleotide metabolism	2	—	—	1	—	—	1	1	—
Phage-associated proteins	—	—	—	1	5	—	1	1	2
Protein folding and degradation	1	1	—	1	1	—	1	1	—
Regulation and cell signaling	8	5	0	4	3	0	9	8	0
Stress survival	3	—	—	1	—	—	3	2	—
Translation	—	—	—	—	—	—	6	1	2

[a] Genes or operons differentially expressed in 35000HPΔ*cpxA* versus 35000HPΔ*cpxR*.
[b] Genes or operons differentially expressed in 35000HPΔ*cpxA* versus 35000HP.
[c] Genes or operons differentially expressed in 35000HPΔ*cpxR* versus 35000HP.
[d] —, no genes or operons were found to be differentially expressed.

TABLE 4 Genes or operons differentially expressed by activation or inactivation of the *H. ducreyi* Cpx 2CST system in the stationary phase

Function and gene identification code[a]	Gene(s)[b]	Description or homolog[c]	Fold change[d]		
			35000HP-Δ*cpxA*/ 35000HP-Δ*cpxR*[e]	35000HP-Δ*cpxA*/ 35000HP[f]	35000HP-Δ*cpxR*/ 35000HP[g]
Amino acid biosynthesis					
HD0577	*selD*	Selenide, water dikinase	−2.2		
HD0890-2[h]	*argC*, *argB*	*N*-Acetyl-γ-glutamyl-phosphate reductase	2.3	2.1	
HD0896	*cysK*	*O*-Acetylserine sulfhydrylase	−7.2	−5.7	
Cell surface structures and associated proteins					
Lipooligosaccharide biosynthesis					
HD0450-4[h]	*waaA*	3-Deoxy-D-manno-octulosonic-acid transferase	2.1		−2.1
HD0653	*waaF*	ADP-heptose-LPS[i] heptosyltransferase II	−2.3	−2.3	
HD1665		D,D-Heptose 1,7-bisphosphate phosphatase	−4.3	−3.6	
OMPs					
HD0045	*momp*	Major OMP	17.9	7.2	−2.6
HD0046-8[h]	*ompA2*, *HD0047*, *HD0048*	Major OMP, OmpA2	−30.5	−25.6	
HD0651-2[h]	*oapA*, *oapB*	Opacity-associated protein A		−2.2	
HD0746	*dltA*	Endo-1,4-β-xylanase A		−2.8	−2.5
HD0769	*dsrA*	Serum resistance protein DsrA	−40.4	−27.4	
HD1017		24-kDa OMP; MltA-interacting MipA protein	−5.7	−3.9	
HD1077-8[h]	*ompP1*	OMP P1	−2.3	−2.7	
HD1155-6[h]	*lspB*, *lspA2*	Large supernatant protein exporter		−15.4	
HD1170	*ompP4*	OMP P4	−2.1		
HD1278-80[h]	*HD1278*, *HD1280*	Serine protease	−3.7	−3.0	
HD1326	*hhdB*	Hemolysin activation/secretion protein	−20.1	−16.9	
HD1327	*hhdA*	Hemolysin	−3.1	−2.4	
HD1433	*ompP2*A	OMP P2-like protein	−9.8	−11.2	
HD1435	*ompP2*B	OMP P2-like protein	13.1	15.9	
HD1856		Possible OMP	−5.2	−5.5	
HD1920	*ncaA*	NcaA class II, necessary for collagen adhesion	−8.8	−7.2	
HD2025	*hgbA*	Hemoglobin-binding protein HgbA	−3.3	−2.6	
Sialyltransferases, HD0685-6[h]	*neuA*, *lst*	Acylneuraminate cytidylyltransferase	2.2		
Type I fimbriae, HD0281-5[h]	*fimA*, *fimB*, *fimC*, *fimD*, *fimE*	Fimbrial major pilin protein	9.8	9.9	
Type IVa pili/type II secretion/competence					
HD0182-5[h]	*HD0182*, *HD0183*, *HD0184*, *HD0185*	Prepilin peptidase dependent protein A	−20.1	−2.2	8.8
HD0209	*comF*	Competence protein F	−2.7		2.5
HD0427-34[h]	*comA*, *HD0428*, *HD0429*, *HD0430*, *HD0431*, *HD0432*, *HD0433*, *comE*	Competence protein A-like protein	−10.8		5.6
HD0650	*comEA*	DNA uptake protein/type II secretion protein	−5.1		4.2
HD0732	*radC*	DNA repair protein RadC	−5.2		5.0
HD1123-6[h]	*pilA*, *pilB*, *pilC*, *pilD*	Prepilin peptidase dependent protein D	−54.0	−4.3	12.3
HD1256	*rec2*	Recombination protein 2	−10.2		5.9
HD1888	*smf*	DNA processing chain A	−3.3		3.2
HD1921	*recG*	ATP-dependent DNA helicase RecG	−2.5	−2.3	
HD1985		DNA transformation protein, T(foX)/Sxy	−9.5	−6.6	
Flp pili and associated proteins, HD1298-312[h]	*flp1*, *flp2*, *flp3*, *orfBC*, *rcpAB*, *orfD*, *tadABCDEFG*	*flp* operon protein Flp1	−35.0	−31.3	

Cell wall biosynthesis and remodeling, HD1400		Soluble lytic murein transglycosylase	2.5		
Cofactor biosynthesis					
HD1389-92[h]	*moaA*, *moaC*, *moaD*, *moaE*	Molybdenum cofactor biosynthesis protein A	−2.8	−3.2	
HD1480	*bioD*	Dithiobiotin synthetase	−2.5		
HD1495		Putative dithiobiotin synthetase	−2.3	−2.4	
HD1874	*ubiF*	2-Octaprenyl-3-methyl-6-methoxy-1,4-benzoquinol hydroxylase	−3.5		2.9
Degradation/assimilation/utilization, HD1857	*ulaD*	3-Keto-L-gulonate-6-phosphate decarboxylase	−2.0		
Fatty acid biosynthesis, HD0181	*fabA*	3-Hydroxydecanoyl-ACP dehydratase	3.6	2.3	
Generation of precursor metabolites and energy					
ATP synthase, HD0003-11[h]	*HD0003*, *atpB*, *atpE*, *atpF*, *atpH*, *atpA*, *atpG*, *atpD*, *atpC*	ATP synthase F0F1 subunit A	−7.6	−6.5	
Anaerobic respiration					
HD0084	*lldD*	L-Lactate dehydrogenase	−9.8	−11.6	
HD0344-47[h]	*nrfA*, *nrfB*	Cytochrome c_{552}	−2.2	−2.7	
HD1110-12[h]	*fdhE*[i]	Formate dehydrogenase accessory protein FdhE	3.1	3.8	
HD1393-4[h]	*torY*, *torZ*	Cytochrome *c*-type protein TorY	−2.7	−2.4	
HD1456-7[h]	*ackA*	Acetate kinase	−2.4		
HD1986	*fumC*	Fumarate hydratase	−3.6	−3.0	
Lipid biosynthesis, HD1253	*dgkA*	Diacylglycerol kinase		−2.0	
Membrane transport/uptake					
HD0025	*dcuB1*	Anaerobic C4-dicarboxylate transporter	2.5		
HD0313-6[h]	*dppB*	Dipeptide transport system permease	2.0	2.3	
HD0614	*kefB*	Glutathione-regulated K^+ efflux system protein	2.6	2.5	
HD0766-8[h]	*manX*, *manY*, *manZ*	Phosphotransferase system mannose-specific transporter subunit IID	2.0	2.3	
HD0790	*ccmD*	Heme exporter protein D	−2.2		
HD1074	*potD2*	Spermidine/putrescine-binding periplasmic protein	2.2		
HD1109		Oxalate/formate antiporter	7.6	7.9	
HD1146	*glpF*	Glycerol uptake facilitator protein	3.3	3.0	
HD1540-6[h]	*HD1546*[i]	Putative ABC transporter			−2.8
HD1639		Major facilitator superfamily transporter	4.7	5.3	
HD1814-5[h]	*HD1814*	Transporter/inner membrane protein YccA			−2.2
HD1859-60[h]	*HD1859*[i]	Phosphotransferase system enzyme IIA permease	−3.3	−2.8	
Nucleoside and nucleotide metabolism, HD0888-9[h]	*deoC*, *deoD*	Deoxyribose-phosphate aldolase	2.6	2.5	

(Continued on following page)

TABLE 4 (Continued)

Function and gene identification code[a]	Gene(s)[b]	Description or homolog[c]	Fold change[d]		
			35000HP-Δ*cpxA*/ 35000HP-Δ*cpxR*[e]	35000HP-Δ*cpxA*/ 35000HP[f]	35000HP-Δ*cpxR*/ 35000HP[g]
Phage-associated proteins					
HD0111		Mu-like phage C protein	2.0		
HD0531-8[h]	*HD1535*[i]	Tail assembly protein			7.7
HD1537-9[h]	*HD1538*[i]	Putative phage-related DNA-binding protein		−2.6	−2.4
Protein folding and degradation, HD1900	*fkpA*	FK506-binding protein-type peptidyl prolyl isomerase	−4.4	−3.2	
Regulation and cell signaling					
HD0261-2[h]	*argR*, *HD0261*	Arginine repressor ArgR	3.4	3.0	
HD0280		Putative GrlR family protein	8.8	8.9	
HD0589-93[h]	*HD0591*[i]	LemA protein; GacS homolog	−2.5	−3.8	
HD0664-5[h]	*HD0665*	LysM domain/BON superfamily protein	2.5		
HD0738	*crp*	Cyclic AMP regulatory protein	3.2	2.5	
HD0910-11[h]	*hicA*, *hicB*	HicA protein	−2.2	−2.6	
HD1028-31[h]	*gcvA*, *HD1029*	DNA-binding transcriptional activator GcvA	−7.1	−5.1	
HD1096		DNA-binding helix-turn-helix protein	−3.0	−2.6	
HD1641-2[h]	*purR*	DNA-binding transcriptional repressor PurR	−2.8	−2.8	
Stress survival					
HD0848	*sodC*	Superoxide dismutase [Cu-Zn]	−2.8	−2.4	
HD1665-8[h]	*bcp*[i], *queF*	Thioredoxin-dependent thiol peroxidase	−3.0	−2.3	
HD1754-5[h]	*ftnA*	Ferritin	−2.1		
Translation					
HD0223-6[h]	*miaB*	(Dimethylallyl)adenosine tRNA methyl-thiotransferase	−2.3		
HD0318-9[h]	*HD0318*, *rlmN*	rRNA large subunit methyltransferase N	−7.5		5.4
HD0448-9[h]	*dusB*, *fis*	Dehydrogenase; tRNA-dihydrouridine synthase B	−2.9	−2.3	
HD1405-7[h]	*efp*	Elongation factor P	−2.3		
HD1257-8[h]	*queA*[i]	*S*-Adenosylmethionine-tRNA ribosyltransferase-isomerase	−4.6		3.5
HD1664		tRNA/rRNA methyltransferase	−2.2		

[a] Does not include genes or operons that encode hypothetical proteins.
[b] For genes that are members of a putative or known operon, only the differentially regulated genes are listed (ordered in the direction of transcription).
[c] For genes that are members of a putative or known operon, the description corresponds to the first gene in the operon.
[d] For genes that are members of a putative or known operon, the fold change corresponds to the first gene in the operon.
[e] Genes or operons differentially regulated in 35000HPΔ*cpxA* versus 35000HPΔ*cpxR*.
[f] Genes or operons differentially regulated in 35000HPΔ*cpxA* versus 35000HP.
[g] Genes or operons differentially regulated in 35000HPΔ*cpxR* versus 35000HP.
[h] Putative or known *H. ducreyi* operons.
[i] Only genes located internal to the operon or toward the 3′ end of the operon were found to be differentially regulated; the description and the fold change correspond to the 5′ gene in the operon that was differentially regulated.
[j] LPS, lipopolysaccharide.

enzymes involved in the assembly of cell surface structures (Table 4; see Table S3 in the supplemental material). Many of these genes and operons were discussed in the virulence determinant section (Table 2). The Cpx 2CST system also downregulated the expression of homologues of two genes that encode serine protease autotransporters (*HD1278* and *HD1280*) (Table 4; see Table S3 in the supplemental material) (46). In addition to these genes, activation of the Cpx 2CST system downregulated the expression of *waaF* and *HD1665*, while it upregulated the expression of *waaA*; these genes are involved in the biosynthesis of lipooligosaccharide (Table 4; see Table S3 in the supplemental material). The Cpx 2CST system also downregulated the expression of homologues of genes involved in type IV pilus biogenesis/type II secretion/competence in other organisms (*pilABCD*, *HD0427-comA-HD0428-HD0429-HD0430-HD0431-HD-432-HD0433-HD0434*, *HD0182-HD0183-HD0184-HD0185*, *comF*, *comE*, *radC*, *rec2*, *smf*, and *recG*) and upregulated the expression of homologues of genes or operons involved in the biogenesis of type I fimbriae in other organisms (*fimABCDE*) and (Table 4; see Table S3 in the supplemental material). The majority of these genes were differentially regulated only in the stationary phase (Table 4; see Table S3). Whether type I fimbriae or type IV pili are expressed by *H. ducreyi* is unknown; the regulation of these genes by the Cpx system suggests that their expression and role in virulence should be explored.

Cofactor biosynthesis. The Cpx 2CST system downregulated the expression of homologues of genes involved in the biosynthesis of molybdenum cofactor (*moaACDE*), biotin (*bioD* and *HD1495*), and ubiquinone (*ubiF*) (Table 4; see Table S3 in the supplemental material).

Generation of precursor metabolites and energy. The Cpx 2CST system downregulated the expression of homologues of genes involved in ATP synthesis (*HD0003-atpBEFHAGDC*), anaerobic respiration (*lldD*, *nrfAB*, *torYZ*, and *dcuB1*), the tricarboxylic acid cycle (*fumC*), and degradation of AcP (*ackA*) (Table 4; see Table S3 in the supplemental material). Downregulation of *ackA* should lead to accumulation of AcP and thus foster the accumulation of phospho-CpxR, promoting a positive feedback loop for repression by CpxR. The Cpx 2CST system activated the expression of a homologue of a gene encoding FdhE, which serves as a proofreading chaperone for formate dehydrogenase, an enzyme involved in anaerobic respiration (Table 4; see Table S3).

Membrane transport and uptake. The Cpx 2CST system downregulated the expression of homologues of genes encoding heme transporter (*ccmD*) and L-ascorbate transporter (*HD1859-HD1860*) (Table 4; see Table S3 in the supplemental material). Homologues of genes involved in dipeptide transport (*dppB*), glycerol transport (*glpF*), secondary sugar transport (*manXYZ*), polyamine transport (*potD2*), potassium/proton antiport (*kefB*), and oxalate-dependent generation of proton motive force (*oxlT*) were upregulated by the Cpx 2CST system (Table 4; see Table S3 in the supplemental material).

Protein folding and degradation. The *H. ducreyi* Cpx 2CST system downregulated the expression of a homologue of a gene involved in protein folding (*fkpA*) (Table 4; see Table S3 in the supplemental material). However, the *H. ducreyi* Cpx 2CST system did not affect the expression of homologs of *degP* and *dsbA*, which are upregulated when the system is activated in *E. coli* (30). *H. ducreyi* lacks an obvious homolog of *ppiA*, which is also upregulated upon activation of the system in *E. coli* (30).

Regulation and cell signaling. The Cpx 2CST system downregulated the expression of homologues of genes encoding or predicted to encode the transcriptional activator GcvA (*gcvA*), the transcriptional repressor PurR (*purR*), the toxin-antitoxin system HicAB (*hicAB*), a putative homolog of GacS (*HD0591*), and a putative homolog of DNA-binding helix-turn-helix protein (*HD1096*) (Table 4; see Table S3 in the supplemental material). The Cpx 2CST system upregulated the expression of homologues of genes encoding or predicted to encode the catabolite activator protein Crp (*crp*), a putative LysM domain/BON superfamily protein (*HD0665*), and a putative GrlR family protein (*HD0280*) (Table 4; see Table S3 in the supplemental material).

Stress survival. In addition to *sodC*, activation of the Cpx 2CST system downregulated the expression of *bcp* and *ftnA*, which are involved in oxidative stress defense in other organisms (Table 4; see Table S3 in the supplemental material).

Translation. The Cpx 2CST system downregulated the expression of homologues of many genes involved in protein synthesis (*dusB*, *efp*, *miaB*, *queA*, *queF*, *rlmN*, and *HD1664*), particularly those that are involved in tRNA and rRNA base modification (Table 4; see Table S3 in the supplemental material). Downregulation of the protein synthesis genes by the Cpx 2CST system was observed only in bacteria grown to the stationary phase (Table 4; see Table S3).

Hypothetical proteins. The Cpx 2CST system downregulated the expression of 15 genes or operons predicted to encode hypothetical proteins, while it upregulated the expression of 14 genes or operons predicted to encode hypothetical proteins (see Table S3 in the supplemental material).

Pathway analysis. Pathway enrichment analysis with annotations from both BioCyc and DAVID bioinformatics resources showed that genes encoding proteins involved in ATP synthesis and nucleoside and nucleotide metabolism were enriched among the genes differentially expressed in the *cpxA* mutant compared to 35000HP (data not shown).

***De novo* identification of the CpxR binding motif.** In *E. coli*, the consensus CpxR binding motif is the tandem repeat GTAAA (N_5)GTAAA (Fig. 4A) (13). A *de novo* motif analysis of the 450-bp promoter regions of all upregulated and downregulated targets in the 35000HPΔ*cpxA*-versus-35000HPΔ*cpxR* comparison did not yield any significant motifs. However, analysis of the promoter regions from the downregulated targets identified an extended motif with an expect value of 6.7×10^{-9} (Fig. 4B). The extended motif consisted of two imperfect tandem repeats arranged in opposite orientations and separated by a 3-bp linker (Fig. 4B); each half of the extended motif bore some similarity to the *E. coli* tandem repeat. The first half of the extended motif contained imperfect 5-bp repeats separated by a 5-bp linker, while the second half of the extended motif contained imperfect 5-bp repeats separated by a 6-bp linker (Fig. 4B). However, the extended motif was found in only 10 out of 66 downregulated promoters (Fig. 4C), suggesting that it might not be required for CpxR binding.

Next, we examined whether one tandem repeat was enriched in the downregulated promoters. A genome-wide search with a PSSM derived from the first tandem repeat in the extended motif with a 4- to 6-nucleotide gap (Fig. 4D) showed that this logo was present in the upstream promoter sequences of 51 (77%) of 66 downregulated targets (see Table S6 in the supplemental material), in 131 (64%) of 204 genes or operons

A

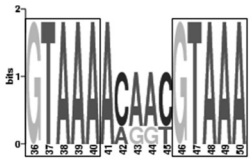

B

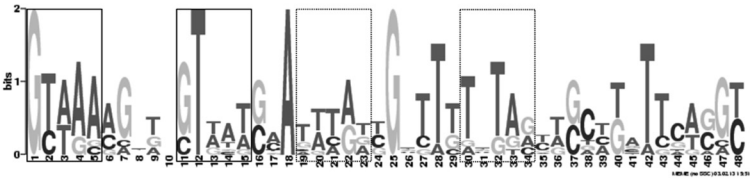

C

Name[a]	Strand[b]	Start[c]	*p*-value[d]	Sites[e]
torY	-	336	7.26×10^{18}	**GTAAA**AGATT**GTTAT**CAA**TATAT**CGTTTT**TCTAC**TTGCCTATTCAGGT
moaA	+	94	7.26×10^{18}	**GTAAA**AGATT**GTTAT**CAA**TATAT**CGTTTT**TCTAC**TTGCCTATTCAGGT
HD0048	-	311	4.52×10^{17}	**GTAAA**AGGTC**GTAAA**CAA**TTAAT**CGCTTG**TTTAG**CACCTGATCGTCGC
ompA2	-	81	1.38×10^{16}	**GTAAA**AGGTC**GTAAA**CAA**TTAAT**CGCTTG**TTTAG**CACCTGATCGTCGT
HD1439	-	243	5.58×10^{13}	**GTTGC**CGTGG**GTGCT**GCA**GTCGG**TGGCTT**TTTAG**TTGTTGCATTGGGC
ulaD	+	49	8.72×10^{13}	**GCTAA**AGTAA**CTAAA**GCA**AATGA**GGTTTT**AATAA**CACCTTCTTCAGGC
HD1668	+	106	1.16×10^{12}	**GCTGG**CGTTG**GTATT**GCA**TTCAG**TGGCAC**GCTAG**GTGCATTTTCAGCC
HD1123	+	198	1.16×10^{12}	**GCAAA**AACGG**CTTAT**GTA**TGTAA**TGATTG**TGGGG**CGGAATATTCTCGC
ccmD	-	34	6.38×10^{12}	**GTAAA**CCTAT**GTGGG**GGA**CTTGG**TGGGTT**TGGGA**TGCGCGGTTAACGT
HD1664	+	44	6.78×10^{12}	**GTTAA**GGCGA**GTTTT**GAA**GATGA**GGCTTT**TGTTA**ATGCAGGTGCAAAT

D

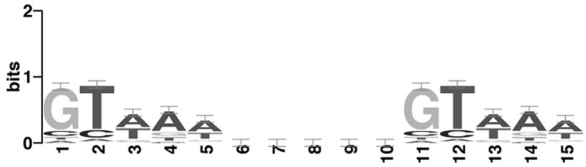

FIG 4 The *H. ducreyi* and *E. coli* CpxR binding motifs. (A) Sequence logo of the *E. coli* CpxR binding sites. The sequence logo was generated with the 450-bp promoter regions from 10 known Cpx target operons (12). The core regions in the motif are boxed. (B) The extended CpxR binding motif in *H. ducreyi*. The extended logo was generated by the MEME algorithm with the 450-bp upstream promoter sequences from the 66 downregulated targets identified in the 35000HPΔ*cpxA*-versus-35000HPΔ*cpxR* comparison in the stationary phase. The putative core regions in the extended motif are boxed. (C) Multiple-sequence alignment of the extended CpxR binding motif in the 10 promoter regions that contained the most significant matches. Superscript letters: a, genes in which the motif was identified; b, location of the extended motif on the template strand (+) or the complementary strand (−); c, start position of the binding site relative to the ATG start codon; d, *P* value for the extended motif; e, sequence of the predicted motif with the putative core regions in bold. (D) Sequence logo of *H. ducreyi* CpxR recognition weight matrix. The matrix frequency of a single GTAAA repeat is obtained by averaging the two parts of the first tandem repeat shown in Fig. 4B. The same nucleotide frequency was used for both GTAAA repeats. The 5-bp linker was assigned with a background frequency that was given by the MEME algorithm.

whose expression levels were less than 2-fold downregulated ($P = 0.03$; odds ratio, 2), and in 395 (55%) of 718 genes or operons whose expression levels were not differentially regulated ($P < 0.001$; odds ratio, 3). Searches for enrichment of the single tandem repeat in the upregulated genes did not reveal any significant matches. The promoter regions of *HD0182*, *HD0427*, *HD1123*, *lspB*, and *dsrA*, which regulated the GFP reporter in response to Cpx activation, contained the CpxR logo (Fig. 4D), while the promoter regions of *fis*, *fimA*, and *HD1278*, which did not regulate the GFP reporter, did not (Fig. 3). These data suggest that the Cpx 2CST system probably directly regulates the majority of the downregulated targets by recognizing one tandem repeat and indirectly regulates the upregulated targets; the significance of the extended motif is unclear.

Site-directed mutagenesis confirms the predicted CpxR binding motif. Activation of the Cpx 2CST system by deletion of *cpxA* downregulates *lspB* expression, and recombinant CpxR binds to the *lspB* promoter region (18). Therefore, we used the reporter plasmid containing the *lspB* promoter sequences to validate the predicted CpxR binding site. With the PSSM derived from the first tandem repeat (Fig. 4D), the *lspB* promoter region in pKF1 was predicted to contain four CpxR binding motifs (see Table S6 in the supplemental material). To identify which of these motifs was required for CpxR binding, we mutagenized the first two nucleotides in the first 5-bp repeat of each binding motif separately (Fig. 5A), introduced the mutagenized plasmids into the *cpxA* and the *cpxR* mutants, and measured the GFP-to-PAL expression ratio. Repression of *lspB* promoter activity in the *cpxA* mutant was significantly relieved by mutagenesis of the first two nucleotides in motif 4 (Fig. 5B and C). However, mutations in motifs 1, 2, and 3 did not relieve the repression of the *lspB* promoter (Fig. 5B and C). Taken together, these data suggest that motif 4 constitutes the binding site for CpxR in the *lspB* promoter and that CpxR likely uses the predicted binding logo (Fig. 4D) to control its direct targets.

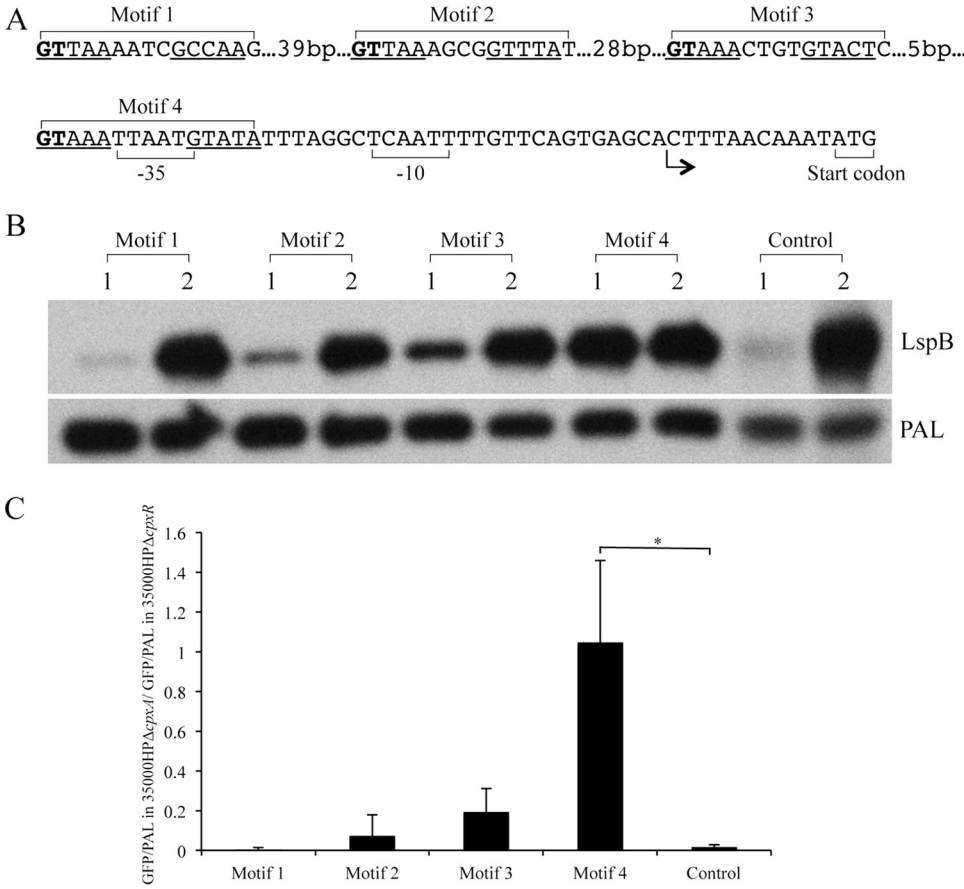

FIG 5 The predicted CpxR binding logo is required for *lspB* promoter activity. (A) *lspB* promoter region showing the locations of the predicted CpxR binding motifs and the locations of the mutagenized nucleotides. Predicted CpxR binding motifs 1 to 4 are indicated, and the mutagenized nucleotides in the binding sites are in bold. The ATG start codon, the transcriptional start site (arrow) determined on the basis of the RNA-Seq data, and the predicted −10 and −35 regions are also indicated. (B) Effect of site-directed mutagenesis of the predicted CpxR binding sites on *lspB* promoter activity measured in the GFP reporter assay. Plasmids containing the wild-type and mutagenized *lspB* promoters were electroporated into the *cpxA* and *cpxR* mutants. Whole-cell lysates were probed with an anti-GFP monoclonal antibody and anti-PAL monoclonal antibody 3B9, which served as a loading control. Motif 1, motif 2, motif 3, and motif 4, reporters with nucleotide substitutions in each respective motif; control, reporter containing the wild-type *lspB* promoter region. Lane 1, *cpxA* mutant, lane 2, *cpxR* mutant. (C) Densitometry analysis of the Western blot assays in panel B. The GFP/PAL ratio in 35000HPΔ*cpxA* is expressed relative to that in 35000HPΔ*cpxR*, which was set to a value of 1. The data are means ± standard deviations from three independent experiments. *, $P = 0.0123$.

DISCUSSION

A previous microarray analysis showed that activation of CpxR by deletion of *cpxA* directly downregulates transcription and expression of several major virulence determinants (18). Consistent with these findings, an *H. ducreyi cpxA* deletion mutant is avirulent in humans (20). To better understand the role of the Cpx 2CST system in controlling virulence, we used RNA-Seq to further define genes potentially regulated by the Cpx 2CST system in *H. ducreyi* at different phases of growth. We showed that activation of the Cpx 2CST system downregulates the majority of its targets, including known and putative virulence factors. These data indicate that CpxA functions as a net phosphatase to maintain parental levels of expression of these virulence determinants during infection of humans.

Our RNA-Seq data showed a high correlation in the results obtained from biological replicates at different phases of growth. The fold changes derived from the RNA-Seq data were generally concordant with the fold changes derived from qRT-PCR. Reporter assays of selected Cpx target promoters further corroborated the transcriptome data.

By comparing the transcriptome of a *cpxA* mutant to that of its parent in the mid-log phase with a 2-fold change cutoff and $P \leq 0.05$, a previous microarray analysis identified 165 genes that are differentially regulated by activation of CpxR (18). Of these 165 genes, 98 (68%) are upregulated, while 67 (32%) are downregulated. In the microarray study, the differentially regulated genes were not grouped by operon structure. Examination of our data obtained from the comparison of the *cpxA* mutant to its parent in the mid-log phase showed that 82 individual genes were differentially regulated. Of these 82 genes, only 17 (21%) were upregulated, while 65 (79%) were downregulated. In *H. ducreyi*, *cpxA* is contained in an operon whose gene order is *mazG*, *cpxR*, *cpxA*, and *HD1471*. The *cpxA* mutant used in the microarray study is an in-frame insertion/deletion mutant, while the *cpxA* mutant used in the RNA-Seq study is an in-frame, unmarked deletion mutant; since both mutants are in frame, they should have no effect on the transcription of *HD1471* (20). The two studies used different media to grow the strains. We do not know if the differences in the results reflect the differences in the sensitivities of the techniques or differences in the strains and growth conditions.

In our study, activation of the *H. ducreyi* Cpx 2CST system by deletion of *cpxA* downregulated nearly 70% of its targets, including *dsrA*, *hgbA*, *lspB-lspA2*, *ncaA*, *flp1-3*, and *tadA*. We previously demonstrated that mutants in these genes were fully attenuated for virulence in humans (6, 34). Thus, attenuation of the *cpxA* mutant in humans is likely a consequence of downregulation of multiple virulence determinants. The *H. ducreyi* Cpx 2CST system also highly downregulated the expression of 15 genes or operons encoding hypothetical proteins and 24 genes in 11 operons encoding homologues of proteins involved in the biogenesis of type IV pili/type II secretion/competence in other organisms. The majority of the type IV pilus/type II secretion/competence genes were differentially regulated only in bacteria grown to the stationary phase and were not identified in the previous microarray analysis, which was performed with bacteria grown to the mid-log phase. Type IV pili are important for adherence, twitching motility, competence, and virulence in other organisms (47). *H. ducreyi* is not naturally competent (48); whether type IV pili are expressed by *H. ducreyi* is unclear. The regulation of these genes by the Cpx system suggests that their expression and role in virulence should be explored.

Unlike deletion of *cpxA*, deletion of *cpxR* differentially regulated only 23 genes or operons in stationary phase; 61% of these genes were upregulated. Deletion of *cpxR* did not affect the expression of any known virulence determinants, except for upregulation of *lspB-lspA2* and downregulation of *dltA*; this is consistent with the observation that a *cpxR* mutant is fully virulent in humans (21). Given that deletions of *cpxA* and *cpxR* yield opposing behaviors with regard to virulence, the findings of this study indicate that activation of the Cpx 2CST system represses *H. ducreyi* virulence determinants and that phosphatase activity of CpxA is critical for *H. ducreyi* to establish and maintain infection in the human host.

Activation of the *H. ducreyi* Cpx 2CST system by deletion of *cpxA* downregulated the expression of homologues of many genes involved in protein synthesis, anaerobic respiration, and ATP synthesis. However, the *H. ducreyi cpxA* mutant showed growth kinetics similar to those of the parental strain. Consistent with this finding, activation of the Cpx 2CST system upregulated the expression of homologues of many genes involved in alternative metabolic, respiratory, and energy-generating pathways, including secondary sugar transport (*manXYZ*) (49), glycerol uptake (*glpF*) (50), dipeptide transport (*dppBCDF*) (51), anaerobic fumarate respiration (*dcuB1*, *aspA*) (52, 53), and oxalate/formate-dependent energy generation (*oxlT*) (54). Given that the activation of the Cpx 2CST system leads to repression of canonical respiratory and energy-generating pathways, we speculate that the upregulation of homologues of genes involved in alternative metabolic, respiratory, and energy-generating pathways probably reflects a compensatory response to maintain energy homeostasis and cell viability.

The *H. ducreyi* CpxA and CpxR proteins are 42 and 60% identical to their *E. coli* homologues, respectively. In *E. coli*, a variety of signals activate the Cpx 2CST system; the majority of these signals involve misfolded proteins in the periplasm as the common stimulus for activation (11). In *H. ducreyi*, the signals that activate the Cpx 2CST system are undefined. Deletion of *H. ducreyi mtrC* activates the Cpx 2CST system; the lack of MtrC may lead to accumulation of toxic products in the periplasm, which induces envelope stress and activates the system (55). In response to membrane stress, the *E. coli* Cpx 2CST system upregulates the expression of many genes involved in envelope protein folding and degradation, including *degP* and *dsbA*, downregulates inner membrane proteins, and coordinates with other regulators of the cell envelope (10, 12). However, consistent with a previous microarray analysis (18), activation of the *H. ducreyi* Cpx 2CST system did not affect the expression of *degP* and *dsbA* and had variable effects on the differential expression of inner membrane proteins. Thus, whether and how the *H. ducreyi* Cpx 2CST system controls envelope stress is unclear (18).

The *E. coli* Cpx 2CST system is activated upon entry into the stationary phase and by signals related to growth and metabolism (16). Comparison of the transcriptomes of the parent and *cpxR* mutant strains showed that the *H. ducreyi* Cpx 2CST system is partially activated in the parent at all growth phases, with maximal activation in the stationary phase. Specifically, the *H. ducreyi* Cpx 2CST system upregulated the expression of homologues of genes involved in relieving protein translocation stress (*yccA*), anaerobic respiration (*dcuB1*), polyamine metabolism (*potD2*), sulfur metabolism (*HD1815*), xylan utilization (*HD0746*), membrane integrity (*momp*), and lipooligosaccharide biosynthesis (*waaA*). The functional significance of the products of these genes in *H. ducreyi* is unknown. Given that the products of the majority of these genes are involved in basic cellular functions, the partial activation of the Cpx 2CST system in the parent probably reflects a physiological role for the system in *H. ducreyi* growth and metabolism.

Using the promoter regions from the downregulated genes identified in our study, we defined a putative *H. ducreyi* CpxR binding motif that is similar to the tandem repeat motif identified in *E. coli* (13). Genome-wide motif analysis showed that the *H. ducreyi* imperfect tandem repeat was enriched in the downregulated genes but not in upregulated genes, suggesting that the upregulated genes are regulated indirectly by CpxR in *H. ducreyi*. Site-directed mutagenesis showed that the tandem repeat motif is required for CpxR regulation of *lspB* promoter sequences. These findings suggest that the single tandem repeat motif is sufficient for CpxR binding.

We conclude that activation of the Cpx 2CST system serves primarily to repress its targets in *H. ducreyi*, including several major virulence determinants, and that CpxA phosphatase activity is critical for *H. ducreyi* to establish and maintain infection in the human host. Future studies will focus on characterizing the direct targets of CpxR and their contributions to *H. ducreyi* pathogenesis.

ACKNOWLEDGMENTS

This work was supported by grant AI27863 to S.M.S. from the National Institutes of Allergy and Infectious Diseases (NIAID). We have no relevant financial relationships to disclose.

We thank Margaret Bauer and David Nelson for their thoughtful criticism of the manuscript and the Hanson laboratory for sharing strains and plasmids.

REFERENCES

1. **Steen R.** 2001. Eradicating chancroid. Bull. World Health Organ. **79:**818–826.
2. **Spinola SM.** 2008. Chancroid and *Haemophilus ducreyi*, p 689–699. *In* Holmes KK, Sparling PF, Stamm WE, Piot P, Wasserheit JN, Corey L, Cohen MS, Watts DH (ed), Sexually transmitted diseases, 4th ed. McGraw-Hill, New York, NY.
3. **McBride WJ, Hannah RC, Le Cornec GM, Bletchly C.** 2008. Cutaneous chancroid in a visitor from Vanuatu. Australas. J. Dermatol. **49:**98–99.

4. **Peel TN, Bhatti D, De Boer JC, Stratov I, Spelman DW.** 2010. Chronic cutaneous ulcers secondary to *Haemophilus ducreyi* infection. Med. J. Aust. **192:**348–350.
5. **Ussher JE, Wilson E, Campanella S, Taylor SL, Roberts SA.** 2007. *Haemophilus ducreyi* causing chronic skin ulceration in children visiting Samoa. Clin. Infect. Dis. **44:**e85–e87.
6. **Janowicz DM, Ofner S, Katz BP, Spinola SM.** 2009. Experimental infection of human volunteers with *Haemophilus ducreyi*: fifteen years of clinical data and experience. J. Infect. Dis. **199:**1671–1679.
7. **Bauer ME, Goheen MP, Townsend CA, Spinola SM.** 2001. *Haemophilus ducreyi* associates with phagocytes, collagen, and fibrin and remains extracellular throughout infection of human volunteers. Infect. Immun. **69:**2549–2557.
8. **Bauer ME, Townsend CA, Ronald AR, Spinola SM.** 2006. Localization of *Haemophilus ducreyi* in naturally acquired chancroidal ulcers. Microbes Infect. **8:**2465–2468.
9. **Raivio TL, Silhavy TJ.** 1997. Transduction of envelope stress in *Escherichia coli* by the Cpx two-component system. J. Bacteriol. **179:**7724–7733.
10. **Vogt SL, Raivio TL.** 2012. Just scratching the surface: an expanding view of the Cpx envelope stress response. FEMS Microbiol. Lett. **326:**2–11.
11. **Hunke S, Keller R, Muller VS.** 2012. Signal integration by the Cpx-envelope stress system. FEMS Microbiol. Lett. **326:**12–22.
12. **Raivio TL, Leblanc SK, Price NL.** 2013. The *Escherichia coli* Cpx envelope stress response regulates genes of diverse function that impact antibiotic resistance and membrane integrity. J. Bacteriol. **195:**2755–2767.
13. **De Wulf P, McGuire AM, Liu X, Lin ECC.** 2002. Genome-wide profiling of promoter recognition by the two-component response regulator CpxR-P in *Escherichia coli*. J. Biol. Chem. **277:**26652–26661.
14. **Price NL, Raivio TL.** 2009. Characterization of the Cpx regulon in *Escherichia coli* strain MC4100. J. Bacteriol. **191:**1798–1815.
15. **Bury-Mone S, Nomane Y, Reymond N, Barbet R, Jacquet E, Imbeaud S, Jacq A, Bouloc P.** 2009. Global analysis of extracytoplasmic stress signaling in *Escherichia coli*. PLoS Gen. **5:**e1000651. doi:10.1371/journal.pgen.1000651.
16. **Wolfe AJ, Parikh N, Lima BP, Zemaitaitis B.** 2008. Signal integration by the two-component signal transduction response regulator CpxR. J. Bacteriol. **190:**2314–2322.
17. **Lima BP, Thanh Huyen TT, Basell K, Becher D, Antelmann H, Wolfe AJ.** 2012. Inhibition of acetyl phosphate-dependent transcription by an acetylatable lysine on RNA polymerase. J. Biol. Chem. **287:**32147–32160.
18. **Labandeira-Rey M, Brautigam CA, Hansen EJ.** 2010. Characterization of the CpxRA regulon in *Haemophilus ducreyi*. Infect. Immun. **78:**4779–4791.
19. **Labandeira-Rey M, Mock JR, Hansen EJ.** 2009. Regulation of expression of the *Haemophilus ducreyi* LspB and LspA2 proteins by CpxR. Infect. Immun. **77:**3402–3411.
20. **Spinola SM, Fortney KR, Baker B, Janowicz DM, Zwickl B, Katz BP, Blick RJ, Munson RS, Jr.** 2010. Activation of the CpxRA system by deletion of *cpxA* impairs the ability of *Haemophilus ducreyi* to infect humans. Infect. Immun. **78:**3898–3904.
21. **Labandeira-Rey M, Dodd D, Fortney KR, Zwickl B, Katz BP, Janowicz DM, Spinola SM, Hansen EJ.** 2011. A *Haemophilus ducreyi cpxR* deletion mutant is virulent in human volunteers. J. Infect. Dis. **203:**1859–1865.
22. **Li H, Durbin R.** 2010. Fast and accurate long-read alignment with Burrows-Wheeler transform. Bioinformatics **26:**589–595.
23. **Breese MR, Liu Y.** 2013. NGSUtils: a software suite for analyzing and manipulating next-generation sequencing datasets. Bioinformatics **29:**494–496.
24. **Robinson MD, McCarthy DJ, Smyth GK.** 2010. edgeR: a Bioconductor package for differential expression analysis of digital gene expression data. Bioinformatics **26:**139–140.
25. **Benjamini Y, Hochberg Y.** 1995. Controlling the false discovery rate: a practical and powerful approach to multiple testing. J. R. Stat. Soc. Ser. B Stat. Methodol. **57:**289–300.
26. **Mao F, Dam P, Chou J, Olman V, Xu Y.** 2009. DOOR: a database for prokaryotic operons. Nucleic Acids Res. **37:**D459–D463.
27. **Keseler IM, Collado-Vides J, Santos-Zavaleta A, Peralta-Gil M, Gama-Castro S, Muniz-Rascado L, Bonavides-Martinez C, Paley S, Krummenacker M, Altman T, Kaipa P, Spaulding A, Pacheco J, Latendresse M, Fulcher C, Sarker M, Shearer AG, Mackie A, Paulsen I, Gunsalus RP, Karp PD.** 2011. EcoCyc: a comprehensive database of *Escherichia coli* biology. Nucleic Acids Res. **39:**D583–590.
28. **Kanehisa M, Goto S.** 2000. KEGG: Kyoto encyclopedia of genes and genomes. Nucleic Acids Res. **28:**27–30.
29. **Caspi R, Altman T, Dreher K, Fulcher CA, Subhraveti P, Keseler IM, Kothari A, Krummenacker M, Latendresse M, Mueller LA, Ong Q, Paley S, Pujar A, Shearer AG, Travers M, Weerasinghe D, Zhang P, Karp PD.** 2012. The MetaCyc database of metabolic pathways and enzymes and the BioCyc collection of pathway/genome databases. Nucleic Acids Res. **40:**D742–753.
30. **Huang da W, Sherman BT, Lempicki RA.** 2009. Systematic and integrative analysis of large gene lists using DAVID bioinformatics resources. Nat. Protoc. **4:**44–57.
31. **Schneider CA, Rasband WS, Eliceiri KW.** 2012. NIH Image to ImageJ: 25 years of image analysis. Nat. Methods **9:**671–675.
32. **Bailey TL, Elkan C.** 1994. Fitting a mixture model by expectation maximization to discover motifs in biopolymers. Proc. Int. Conf. Intell. Syst. Mol. Biol. **2:**28–36.
33. **Liu Y, Taylor MW, Edenberg HJ.** 2006. Model-based identification of *cis*-acting elements from microarray data. Genomics **88:**452–461.
34. **Janowicz DM, Cooney SA, Walsh J, Baker B, Katz BP, Fortney KR, Zwickl B, Ellinger S, Munson RS, Jr.** 2011. Expression of the Flp proteins by *Haemophilus ducreyi* is necessary for virulence in human volunteers. BMC Microbiol. **11:**208. doi:10.1186/1471-2180-11-208.
35. **Labandeira-Rey M, Janowicz DM, Blick RJ, Fortney KR, Zwickl B, Katz BP, Spinola SM, Hansen EJ.** 2009. Inactivation of the *Haemophilus ducreyi luxS* gene affects the virulence of this pathogen in human subjects. J. Infect. Dis. **200:**409–416.
36. **Rinker SD, Gu X, Fortney KR, Zwickl BW, Katz BP, Janowicz DM, Spinola SM, Bauer ME.** 2012. Permeases of the Sap transporter are required for cathelicidin resistance and virulence of *Haemophilus ducreyi* in humans. J. Infect. Dis. **206:**1407–1414.
37. **Gangaiah D, Li W, Fortney KR, Janowicz DM, Ellinger S, Zwickl B, Katz BP, Spinola SM.** 2013. Carbon storage regulator A contributes to the virulence of *Haemophilus ducreyi* in humans by multiple mechanisms. Infect. Immun. **81:**608–617.
38. **Fortney KR, Young RS, Bauer ME, Katz BP, Hood AF, Munson RS, Jr, Spinola SM.** 2000. Expression of peptidoglycan-associated lipoprotein is required for virulence in the human model of *Haemophilus ducreyi* infection. Infect. Immun. **68:**6441–6448.
39. **Mount KL, Townsend CA, Rinker SD, Gu X, Fortney KR, Zwickl BW, Janowicz DM, Spinola SM, Katz BP, Bauer ME.** 2010. *Haemophilus ducreyi* SapA contributes to cathelicidin resistance and virulence in humans. Infect. Immun. **78:**1176–1184.
40. **Bauer ME, Townsend CA, Doster RS, Fortney KR, Zwickl BW, Katz BP, Spinola SM, Janowicz DM.** 2009. A fibrinogen-binding lipoprotein contributes to virulence of *Haemophilus ducreyi* in humans. J. Infect. Dis. **199:**684–692.
41. **Banks KE, Fortney KR, Baker B, Billings SD, Katz BP, Munson RS, Jr, Spinola SM.** 2008. The enterobacterial common antigen-like gene cluster of *Haemophilus ducreyi* contributes to virulence in humans. J. Infect. Dis. **197:**1531–1536.
42. **Bong CTH, Fortney KR, Katz BP, Hood AF, San Mateo LR, Kawula TH, Spinola SM.** 2002. A superoxide dismutase C mutant of *Haemophilus ducreyi* is virulent in human volunteers. Infect. Immun. **70:**1367–1371.
43. **Palmer KL, Thornton AC, Fortney KR, Hood AF, Munson RS, Jr, Spinola SM.** 1998. Evaluation of an isogenic hemolysin-deficient mutant in the human model of *Haemophilus ducreyi* infection. J. Infect. Dis. **178:**191–199.
44. **Janowicz D, Luke NR, Fortney KR, Katz BP, Campagnari AA, Spinola SM.** 2006. Expression of OmpP2A and OmpP2B is not required for pustule formation by *Haemophilus ducreyi* in human volunteers. Microb. Pathog. **40:**110–115.
45. **Spinola SM, Li W, Fortney KR, Janowicz DM, Zwickl B, Katz BP, Munson RS, Jr.** 2012. Sialylation of lipooligosaccharides is dispensable for the virulence of *Haemophilus ducreyi* in humans. Infect. Immun. **80:**679–687.
46. **Ruiz-Perez F, Wahid R, Faherty CS, Kolappaswamy K, Rodriguez L, Santiago A, Murphy E, Cross A, Sztein MB, Nataro JP.** 2011. Serine protease autotransporters from *Shigella flexneri* and pathogenic *Escherichia coli* target a broad range of leukocyte glycoproteins. Proc. Natl. Acad. Sci. U. S. A. **108:**12881–12886.
47. **Burrows LL.** 2012. *Pseudomonas aeruginosa* twitching motility: type IV pili in action. Annu. Rev. Microbiol. **66:**493–520.
48. **Redfield RJ, Findlay WA, Bosse J, Kroll JS, Cameron AD, Nash JH.**

2006. Evolution of competence and DNA uptake specificity in the Pasteurellaceae. BMC Evol. Biol. **6:**82. doi:10.1186/1471-2148-6-82.
49. **Plumbridge J.** 1998. Control of the expression of the *manXYZ* operon in *Escherichia coli*: Mlc is a negative regulator of the mannose PTS. Mol. Microbiol. **27:**369–380.
50. **Beijer L, Nilsson RP, Holmberg C, Rutberg L.** 1993. The *glpP* and *glpF* genes of the glycerol regulon in *Bacillus subtilis*. J. Gen. Microbiol. **139:** 349–359.
51. **Weinberg MV, Maier RJ.** 2007. Peptide transport in *Helicobacter pylori*: roles of Dpp and Opp systems and evidence for additional peptide transporters. J. Bacteriol. **189:**3392–3402.
52. **Janausch IG, Garcia-Moreno I, Unden G.** 2002. Function of DcuS from *Escherichia coli* as a fumarate-stimulated histidine protein kinase *in vitro*. J. Biol. Chem. **277:**39809–39814.
53. **Kleefeld A, Ackermann B, Bauer J, Kramer J, Unden G.** 2009. The fumarate/succinate antiporter DcuB of *Escherichia coli* is a bifunctional protein with sites for regulation of DcuS-dependent gene expression. J. Biol. Chem. **284:**265–275.
54. **Anantharam V, Allison MJ, Maloney PC.** 1989. Oxalate:formate exchange. The basis for energy coupling in *Oxalobacter*. J. Biol. Chem. **264:** 7244–7250.
55. **Rinker SD, Trombley MP, Gu X, Fortney KR, Bauer ME.** 2011. Deletion of *mtrC* in *Haemophilus ducreyi* increases sensitivity to human antimicrobial peptides and activates the CpxRA regulon. Infect. Immun. **79:**2324–2334.
56. **Al-Tawfiq JA, Thornton AC, Katz BP, Fortney KR, Todd KD, Hood AF, Spinola SM.** 1998. Standardization of the experimental model of *Haemophilus ducreyi* infection in human subjects. J. Infect. Dis. **178:**1684–1687.